

Nickel-Catalyzed Intramolecular Alkene Difunctionalization by Ball-Milling

Matthew T. J. Williams,^a Louis C. Morrill,^{a,*} and Duncan L. Browne^{b,*}

^a Cardiff Catalysis Institute, School of Chemistry, Cardiff University, Main Building, Park Place, Cardiff, CF10 3AT, UK
+44 2920875840

E-mail: MorrillLC@cardiff.ac.uk

^b School of Pharmacy, University College London, 29-39 Brunswick Square, Bloomsbury, London, WC1 N 1AX, UK
+44 (0)207 679 5281

E-mail: Duncan.Browne@ucl.ac.uk

Manuscript received: February 24, 2023; Revised manuscript received: April 2, 2023;
Version of record online: April 26, 2023

 Supporting information for this article is available on the WWW under <https://doi.org/10.1002/adsc.202300188>

 © 2023 The Authors. Advanced Synthesis & Catalysis published by Wiley-VCH GmbH. This is an open access article under the terms of the Creative Commons Attribution License, which permits use, distribution and reproduction in any medium, provided the original work is properly cited.

Abstract: A mechanochemical nickel-catalyzed intramolecular difunctionalization reaction of alkene tethered aryl halides with alkyl halides is herein described. This method allows for synthesis of 3,3-disubstituted heterocycles, namely oxindoles, with shorter reaction times than solution-phase counterparts. Additionally, this process is solvent minimized, with DMA used in liquid-assisted grinding (LAG) quantities and circumvents the need for chemical activation of the terminal reductant (manganese) through mechanical grinding. The process can be scaled up to yield over a gram of product and modest enantioinduction is possible by utilizing a chiral PyrOX ligand.

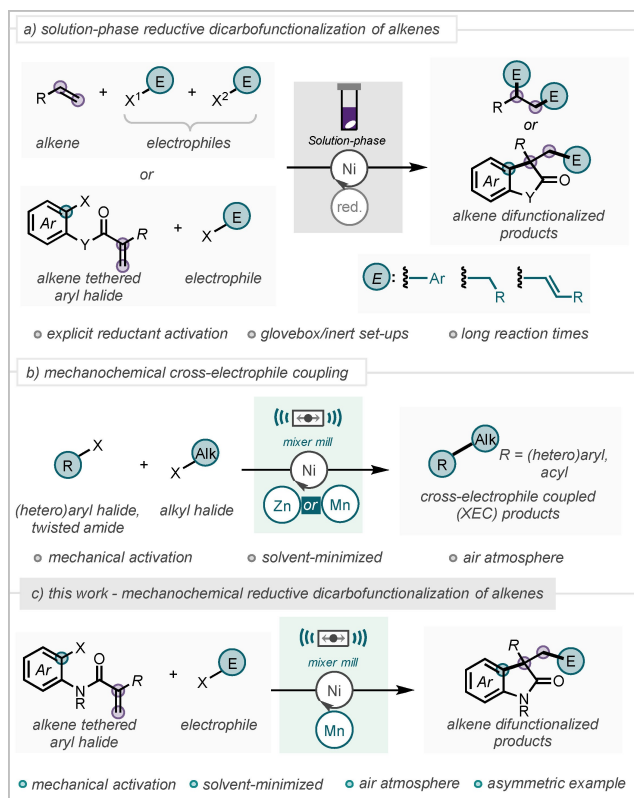
Keywords: Mechanochemistry; Ball-mill; Nickel-catalysis; Solvent-minimized; Heterocycles

Introduction

Reductive cross-coupling processes, such as cross-electrophile coupling (XEC), have seen increased interest in recent years. These processes, in particular XEC, have been pioneered by the likes of Weix and Gong and involve the cross-coupling of two electrophilic species, such as a $C(sp^2)$ halide and a $C(sp^3)$ halide.^[1,2] These XEC processes typically utilize earth abundant nickel as a catalyst and involve a terminal reductant, such as zinc or manganese, to turn over the catalytic cycle. XEC provides a complementary process to traditional palladium-catalyzed cross-coupling, however, with some key advantages, such as the avoidance of nucleophilic substrates (organozincs, Grignards, boronic acids) which can cause issues in late-stage functionalization processes and are often difficult to handle. Similarly, reductive nickel-catalysis has also been applied to the difunctionalization of alkenes, including hydro-carbofunctionalization

and dicarbofunctionalization, also known as conjunctive coupling.^[3,4] Dicarbofunctionalization has received keen interest recently, with both inter- and intramolecular variants of this reactivity being developed.^[5,6]

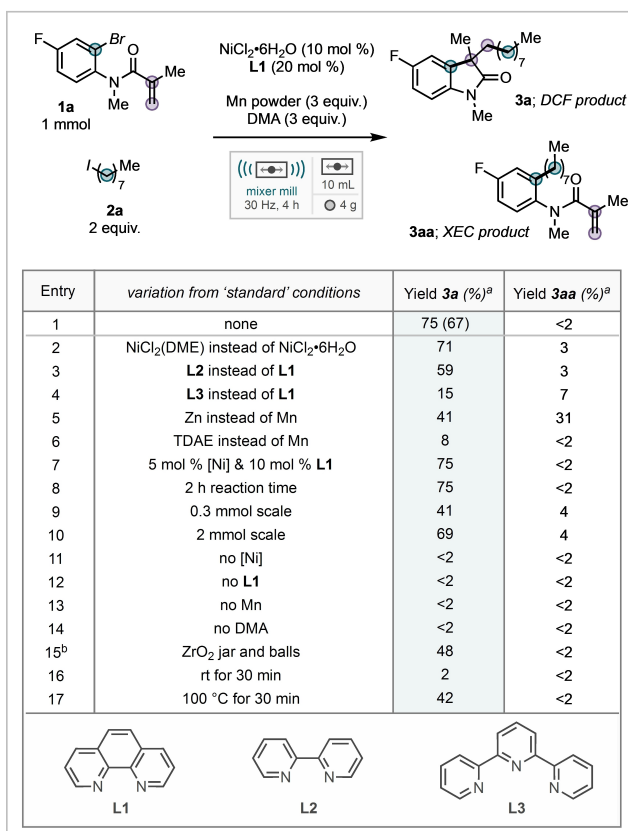
These are strictly three-component reactions (alkene and two electrophiles), however, in the intramolecular variants one of the electrophiles is tethered to the alkene e.g. an alkene tethered aryl halide. The electrophiles are typically $C(sp^2)$ or $C(sp^3)$ species, such as aryl halides, alkyl halides, and alkenyl halides (Scheme 1A). The products from intramolecular difunctionalization processes are cyclized products, such as 3,3-disubstituted oxindoles, indolines, and benzofuranones, which are motifs that can be found in pharmaceutically relevant compounds.^[7] However, these processes, along with other reductive nickel processes such as XEC, suffer from some notable drawbacks, for example the need for a glovebox or inert reaction set-ups, long reaction times, and the tedious



Scheme 1. A) Overview of solution-based intramolecular alkene dicarbofunctionalization, B) Previous work on mechanochemical XEC, C) This work.

requirement to activate the terminal metal reductant. This can be somewhat circumvented by replacing the terminal reductant with a photoredox system.^[8]

Mechanochemistry and ball-milling has shown huge promise in recent years as an alternative synthetic method to traditional solution-based chemistry.^[9,10] This has included its application to cross-coupling chemistry, characterized by reduced reaction times, circumvention of inert reaction set-ups, and reactivity of insoluble substrates.^[11] More recently, the activation of zero-valent metals, such as zinc and manganese, by mechanical grinding has been demonstrated as an additional benefit over solution-phase chemistry.^[12] This has included work from our group where nickel-catalyzed XEC of aryl halides, heteroaryl halides, or *N*-acyl imides/‘twisted amides’, with alkyl halides was successfully carried out under ball-milling conditions (Scheme 1B).^[13] These reports demonstrated significantly reduced reaction times (2 h vs >16 h solution), the use of *N,N*-dimethylacetamide (DMA) in only liquid-assisted grinding (LAG) quantities,^[14] and the avoidance of inert reaction conditions or explicit chemical activation of the terminal reductants (zinc or manganese). Addition-



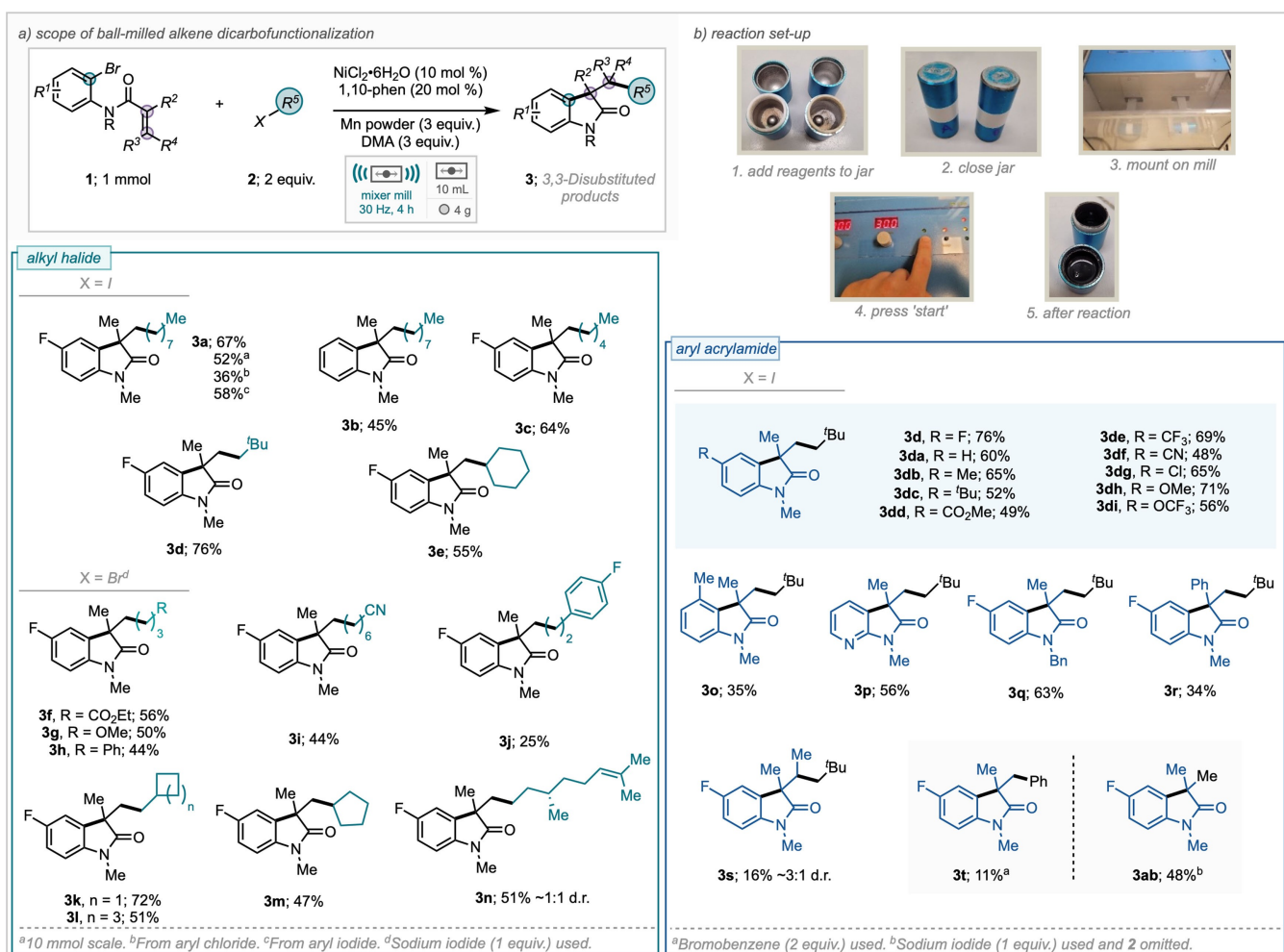
^aYield determined via ¹⁹F NMR analysis of crude reaction mixture using (trifluoromethyl)benzene (0.2036 mmol) as an internal standard. Isolated yields shown in parentheses. ^bConducted in a planetary ball-mill (see Supporting Information for details).

Scheme 2. Reaction optimization - variation from ‘standard’ reaction conditions for model system.

ally, it has been demonstrated that *N*-heterocycles can be synthesized from functionalized alkyl bromides by exploiting piezoelectric materials, such as barium titanate, under mechanochemical conditions.^[15] However, building on our previous work, we envisaged that our methodology could be applied to intramolecular alkene dicarbofunctionalization, providing a facile method to synthesize 3,3-disubstituted heterocyclic compounds, with the established benefits of mechanochemical XEC preserved (Scheme 1C).

Results and Discussion

Our studies commenced with the investigation of a model reaction system, fluoro-substituted aryl acrylamide (**1a**) and 1-iodooctane (**2a**). Initial reactions revealed that the desired dicarbofunctionalization (DCF) product (**3a**) could be formed in 23% isolated yield using $\text{NiCl}_2\cdot 6\text{H}_2\text{O}$ (10 mol %) as the catalyst, 1,10-phenanthroline (20 mol %) as the ligand, zinc (2 equiv.) as the reductant, DMA (3 equiv.) in LAG quantities, with a 2-hour reaction



Scheme 3. Scope of ball-milled alkene dicarbofunctionalization.

time and a 0.3 mmol reaction scale (see Supporting Information for experimental procedures). However, XEC product (**3aa**) was also formed in 22% isolated yield.

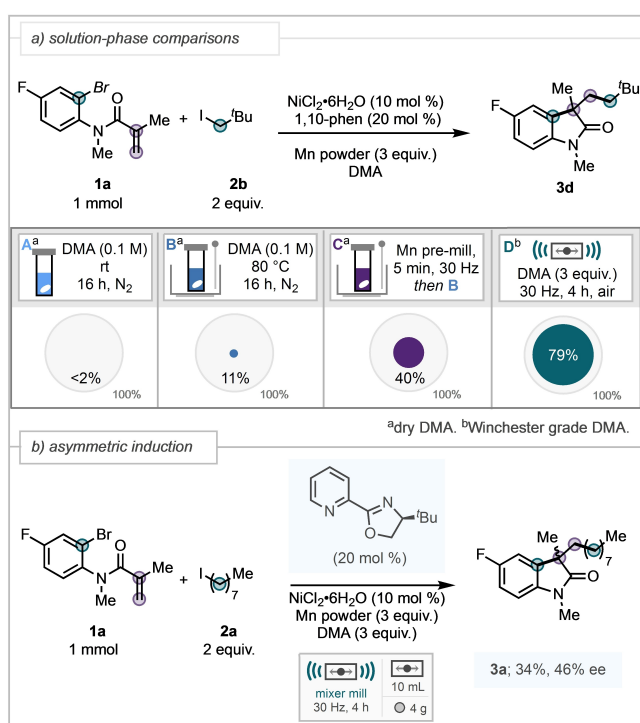
A full reaction optimization was carried out, leading to the following ‘optimal’ conditions; $\text{NiCl}_2 \cdot 6\text{H}_2\text{O}$ (10 mol %) as the catalyst, 1,10-phenanthroline (20 mol %) as the ligand, manganese (3 equiv.) as the reductant, DMA (3 equiv.; 0.28 $\mu\text{L}/\text{mg}$), and a 4-hour reaction time (see Table S1 of Supporting Information for optimization details). Additionally, increasing the reaction scale from 0.3 to 1 mmol had a significant impact on the efficacy of the process. These conditions yielded the desired product (**3a**) in 67% isolated yield, with only trace amounts of the XEC product (**3aa**) observed (Scheme 2, entry 1). Variation from these ‘standard’ conditions, such as changing the catalyst to $\text{NiCl}_2(\text{DME})$, or the ligand to either bipyridine or terpyridine led to a decrease in product yield (entries 2–4). Changing the reductant to zinc

yielded an approximately 1:1 ratio of DCF product **3a** and XEC product **3aa**, and organic reductant tetrakis(dimethylamino)ethylene (TDAE) was largely ineffective (entries 5 and 6). The catalyst loading could be reduced to 5 mol % and the reaction time to 2 hours without sacrificing product yield in the model system (entries 7 and 8), however, initial investigations into the scope of the reaction revealed that 10 mol % of catalyst and a 4 hour reaction time were more effective, hence were maintained as such. Testing the conditions at the original reaction scale of 0.3 mmol gave a lower product yield than at 1 mmol (entry 9). And increasing the scale further to 2 mmol did not lead to an improvement in yield, hence we proceeded with 1 mmol as the optimal reaction scale (entry 10). Control reactions revealed that the process is ineffective in the absence of nickel, ligand, manganese, or DMA (entries 11–14). However, the presence of steel from the milling media is not critical to the reaction success, as 48% NMR yield

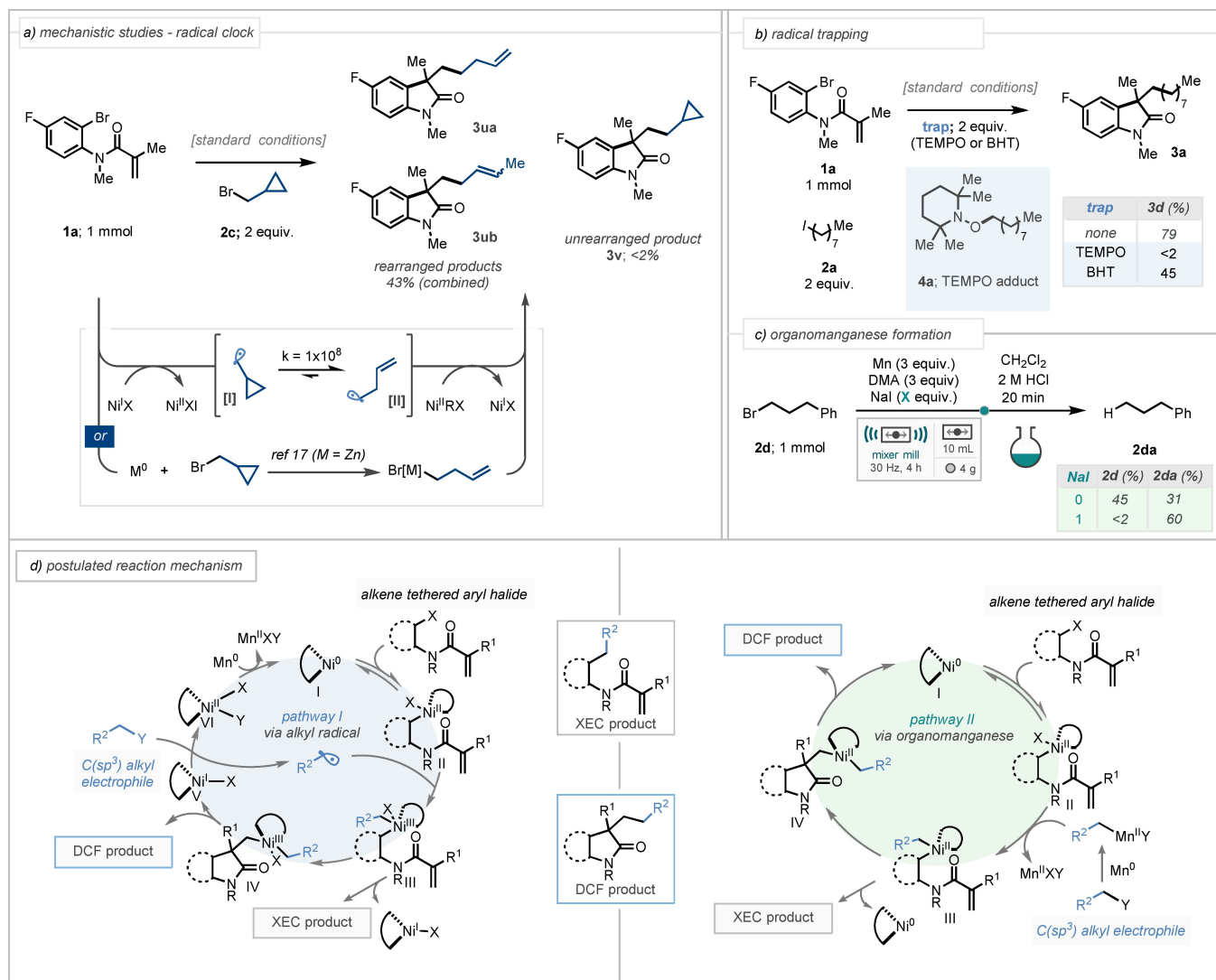
of **3a** was achieved when the reaction was run on a planetary ball-mill with zirconia based milling media (entry 15). This reduction in yield can most likely be attributed to the lower energy forces imparted by the planetary mill compared to a mixer mill. Additionally, the application of heat was shown to improve the product yield on a short timeframe (entries 16 and 17), but the room temperature result coupled with a 2 to 4 hour reaction time was more effective overall. With these conditions in hand, we moved on to investigate the substrate scope of this process (Scheme 3). We demonstrated that the model system could be scaled up 10-fold to yield 1.60 grams of product **3a**, albeit in slightly lower yield, simply by increasing the jar size to 30 mL and the ball size to 12 g. For the coupling with alkyl iodides, it was shown that the chloro and iodo analogues of the model substrate (**1a**) could be employed, furnishing **3a** in 36% and 58% yield, respectively. Other successful alkyl iodides included 1-iodopentane, neopentyl iodide and 1-iodocyclohexane, furnishing **3c**, **3d** and **3e**, respectively, in moderate to good yields. For the coupling with alkyl bromides, it was found that adding an equivalent of sodium iodide was necessary for improved reactivity (see Table S2 of Supporting Information for details).

To this end, alkyl bromides containing an ester, methyl ether, and nitrile groups were successfully

employed to furnish their respective products (**3f**, **3g**, **3h**) in modest yields. Other examples include various cycloalkyl containing products (**3k**–**3m**) and a citronellyl chain (**3n**), which was produced as a 1:1 inseparable mixture of diastereomers. For the alkene tethered aryl bromide portion of the scope, neopentyl iodide was chosen as the coupling partner, as this example gave the highest yield during the alkyl halide scope. To this end, a variety of substitutions on the aromatic ring of the aryl bromide was tolerated, including a methyl ester (**3dd**), trifluoromethyl (**3de**), cyano (**3df**), and methoxy (**3dh**); all in moderate to good yields. Gratifyingly, a chloro-substituted oxindole (**3dg**) could be prepared, without any competing reactivity at the C–Cl site, allowing for further functionalization (cross-coupling) to be carried out. A sterically hindered ortho methylated oxindole (**3o**) could be successfully synthesized, albeit in lower yield, as well as an aza-oxindole (**3p**) in moderate yield. The substitution on the nitrogen could be varied to a benzyl group (**3q**) and the acrylamide moiety could be varied to a phenacrylamide (**3r**) or a dimethyl acrylamide (**3s**) derived from tiglic acid, albeit in lower yields. In the latter case, the product was obtained as an approximately 3:1 inseparable mixture of diastereomers. Additionally, it was shown that an sp^2 – sp^2 coupling is tolerated by employing bromobenzene as the second electrophile, furnishing **3t**, in low yield. Interestingly, when sodium iodide was used as an additive and the second electrophile was omitted, the reductive Heck-type product (**3ab**) could be formed in 48% yield. Some unsuccessful substrates included attempts to synthesize other 3,3,–disubstituted heterocycles, such as benzothiophenone, and attempts to utilize tertiary alkyl halides, such as *tert*-butyl iodide. It can be noted that our developed process is a blended approach i.e., our substrates are synthesized by solution-phase methods and then subjected to the mechanochemical protocol, however, we are able to synthesize our substrate mechanochemically using a previously reported protocol for the direct amidation of esters, albeit in reduced yield (see Supporting Information for details).^[10f] Following this, we carried out solution-phase comparisons analogous to our ball-milled process, as there is no direct comparison available in the literature. Three sets of conditions were performed: A) dry DMA, room temperature, under nitrogen, for 16 hours, B) dry DMA, 80 °C, under nitrogen, for 16 hours, and C) pre-milled manganese (5 min) then conditions B) (Scheme 4A). Only conditions B and C produced any product (**3d**), 11% and 40% by NMR, respectively. These results highlight the requirement to explicitly activate the terminal reductant in these processes. Whereas the ball-milled process pro-



Scheme 4. A) Solution-phase comparisons, B) Asymmetric induction.



Scheme 5. Mechanistic studies: A) Radical clock reaction, B) Organomanganese formation, C) Radical trapping reaction, D) Plausible mechanism.

vides 79% product by NMR after only 4 hours, without the need for heating or dry conditions.

Next, we sought to investigate the potential for enantioinduction, as the oxindole products are chiral. A small screen of common chiral ligands (see Supporting Information for details) revealed that a *tert*-butyl substituted PyrOx ligand could be utilized in place of 1,10-phenanthroline to furnish **3a** in 34% yield and with 46% enantiomeric excess (Scheme 4B). The yield and ee are modest, however, provides a proof-of-concept for enantioselective nickel-catalysis under mechanochemical conditions.

To elucidate the mechanism, a series of experiments were carried out, which would allow the fate of the alkyl halide to be discerned i. e., whether an alkyl radical or organomanganese intermediate is

present. This included using (cyclopropyl)methyl bromide (**2c**) as the alkyl coupling partner, which gave exclusive formation of the rearranged products **3ua** and **3ub** in a 43% combined isolated yield, with no observable amount of the unreacted product **3v** (Scheme 5a). The presence of chain-walked product **3ub** suggests a nickel-hydride intermediate could be present in the mechanism, also.^[16] It is possible that the rearranged products **3ua** and **3ub** could arise from a radical pathway or from an organomanganese intermediate, which has been reported *via* an organozinc reagent.^[17] To probe this further, alkyl bromide **2d** was milled with manganese and DMA for 4 hours followed by an acid quench (Scheme 5c). The hydrolyzed compound **2da** was formed in 31% yield by NMR, demonstrating the potential

to form organomanganese intermediates under these conditions. Running the same reaction with an equivalent of sodium iodide increased the NMR yield of the hydrolyzed compound (**2da**) to 60%. Additionally, radical trapping experiments using 2 equivalents of either 2,2,6,6-tetramethylpiperidine 1-oxyl (TEMPO) or butylated hydroxytoluene (BHT) were carried out (Scheme 5b). The reaction with TEMPO resulted in no product formation, which could suggest the interception of radical intermediates, however the expected TEMPO adduct (**4a**) could not be detected and only starting materials were observed by either NMR or mass spectrometry. The reaction with BHT resulted in a reduced yield of the product (**3a**), 45% by NMR, suggesting that a radical pathway was suppressed. However, we cannot rule out these reductions in yield arising from changes in rheology affecting the mixing efficiency of the reaction mixture.

All of this considered, it appears that our process could follow one of two reaction pathways, one involving a single-electron transfer process to generate an alkyl radical intermediate, or the other *via* an *in situ* generated organomanganese intermediate (Scheme 5d). The pathway involving radical intermediates is generally accepted in solution-phase reports, however, the formation of **3t** during the substrate scope, using bromobenzene as the second electrophile, suggests that an organomanganese pathway could predominate (*cf.* Scheme 3).

Conclusion

In conclusion, a mechanochemical method to synthesize 3,3-distubstituted oxindoles *via* nickel-catalyzed alkene difunctionalization has been developed. This process has good substrate scope and has several key benefits over solution-phase analogues, namely shorter reaction times, no requirement for bulk reaction solvent, inert reaction atmospheres or explicit activation of the terminal reductant (manganese). We also demonstrated that the process is amenable to scale-up and asymmetric induction is possible by utilizing a chiral ligand. Further investigations into the activation of zero-valent metals, such as manganese and zinc, and their application in organic transformations are currently ongoing.

Experimental Section

For optimization data, experimental procedures, and characterization data, see the accompanying Supporting Information (PDF)

Acknowledgements

We gratefully acknowledge the School of Chemistry, Cardiff University for generous support and the EPSRC-funded Bath/Bristol/Cardiff Catalysis Centre for Doctoral Training (M.T.J.W. EP/L016443/1).

References

- [1] For some reviews on cross-electrophile coupling, see; a) D. A. Everson, D. J. Weix, *J. Org. Chem.* **2014**, *79*, 4793–4798; b) D. J. Weix, *Acc. Chem. Res.* **2015**, *48*, 1767–1775; c) J. Gu, X. Wang, W. Xue, H. Gong, *Org. Chem. Front.* **2015**, *2*, 1411–1421; d) D. A. Everson, B. A. Jones, D. J. Weix, *J. Am. Chem. Soc.* **2012**, *134*, 6146–6159.
- [2] For some examples of solution-phase cross-electrophile coupling, see; a) D. A. Everson, R. Shrestha, D. J. Weix, *J. Am. Chem. Soc.* **2010**, *132*, 920–921; b) K. A. Johnson, S. Biswas, D. J. Weix, *Chem. Eur. J.* **2016**, *22*, 7399–7402; c) S. Kim, M. J. Goldfogel, M. M. Gilbert, D. J. Weix, *J. Am. Chem. Soc.* **2020**, *142*, 9902–9907; d) X. Wang, S. Wang, W. Xue, H. Gong, *J. Am. Chem. Soc.* **2015**, *137*, 11562–11565; e) S. Biswas, B. Qu, J. N. Desrosiers, Y. Choi, N. Haddad, N. K. Yee, J. J. Song, C. H. Senanayake, *J. Org. Chem.* **2020**, *85*, 8214–8220.
- [3] For some reviews on nickel-catalyzed alkene difunctionalization, see; a) X. X. Wang, X. Lu, Y. Li, J. W. Wang, Y. Fu, *Sci. China Chem.* **2020**, *63*, 1586–1600; b) Y. C. Luo, C. Xu, X. Zhang, *Chin. J. Chem.* **2020**, *38*, 1371–1394; c) J. Derosa, O. Apolinar, T. Kang, V. T. Tran, K. M. Engle, *Chem. Sci.* **2020**, *11*, 4287–4296; d) K. E. Poremba, S. E. Dibrell, S. E. Reisman, *ACS Catal.* **2020**, *10*, 8237–8246; e) X. Qi, T. Diao, *ACS Catal.* **2020**, *10*, 8542–8556.
- [4] For some examples of alkene dicarbofunctionalization catalyzed by other metals, such as copper and palladium, see; a) K. B. Urkalan, M. S. Sigman, *Angew. Chem. Int. Ed.* **2009**, *48*, 3146–3149; *Angew. Chem.* **2009**, *121*, 3192–3195; b) L. Liao, R. Jana, K. B. Urkalan, M. S. Sigman, *J. Am. Chem. Soc.* **2011**, *133*, 5784–5787; c) F. Wang, D. Wang, X. Mu, P. Chen, G. Liu, *J. Am. Chem. Soc.* **2014**, *136*, 10202–10205; d) Z. Liu, T. Zeng, K. S. Yang, K. M. Engle, *J. Am. Chem. Soc.* **2016**, *138*, 15122–15125; e) L. Wu, F. Wang, X. Wan, D. Wang, P. Chen, G. Liu, *J. Am. Chem. Soc.* **2017**, *139*, 2904–2907.
- [5] For some examples of nickel-catalyzed intermolecular alkene dicarbofunctionalization, see; a) T. Qin, J. Cornella, C. Li, L. R. Malins, J. T. Edwards, S. Kawamura, B. D. Maxwell, M. D. Eastgate, P. S. Baran, *Science* **2016**, *352*, 801–805; b) J. W. Gu, Q. Q. Min, L. C. Yu, X. Zhang, *Angew. Chem. Int. Ed.* **2016**, *55*, 12270–12274; *Angew. Chem.* **2016**, *128*, 12458–12462; c) A. García-Domínguez, Z. Li, C. Nevado, *J. Am. Chem. Soc.* **2017**, *139*, 6835–6838; d) J. Derosa, V. A. Van Der Puyl, V. T. Tran, M. Liu, K. M. Engle, *Chem. Sci.* **2018**, *9*, 5278–5283; e) W. Shu, A. García-Domínguez, M. T. Quirós, R. Mondal, D. J. Cárdenas, C. Nevado, *J. Am.*

Chem. Soc. **2019**, *141*, 13812–13821; f) Z. F. Yang, C. Xu, X. Zheng, X. Zhang, *Chem. Commun.* **2020**, *56*, 2642–2645; g) H. Wang, C. F. Liu, R. T. Martin, O. Gutierrez, M. J. Koh, *Nat. Chem.* **2022**, *14*, 188–195.

[6] For some examples of nickel-catalyzed intramolecular alkene dicarbofunctionalization, see; a) A. Vaupel, P. Knochel, *J. Org. Chem.* **1996**, *61*, 5743–5753; b) V. B. Phapale, E. Buñuel, M. García-Iglesias, D. J. Cárdenas, *Angew. Chem. Int. Ed.* **2007**, *46*, 8790–8795; *Angew. Chem.* **2007**, *119*, 8946–8951; c) S. Kc, P. Basnet, S. Thapa, B. Shrestha, R. Giri, *J. Org. Chem.* **2018**, *83*, 2920–2936; d) K. Wang, Z. Ding, Z. Zhou, W. Kong, *J. Am. Chem. Soc.* **2018**, *140*, 12364–12368; e) Y. Ping, K. Wang, Q. Pan, Z. Ding, Z. Zhou, Y. Guo, W. Kong, *ACS Catal.* **2019**, *9*, 7335–7342; f) Y. Feng, S. Yang, S. Zhao, D. P. Zhang, X. Li, H. Liu, Y. Dong, F. G. Sun, *Org. Lett.* **2020**, *22*, 6734–6738; g) J. Wu, C. Wang, *Org. Lett.* **2021**, *23*, 6407–6411; h) X. Wu, B. Luan, W. Zhao, F. He, X.-Y. Wu, J. Qu, Y. Chen, *Angew. Chem. Int. Ed.* **2022**, *61*, e2021115.

[7] a) Y. Kamano, H.-P. Zhang, Y. Ichihara, H. Kizu, K. Komiyama, G. R. Pettit, *Tetrahedron Lett.* **1995**, *36*, 2783–2784; b) D. J. Triggle, J. M. Mitchell, R. Filler, *CNS Drug Rev.* **1998**, *4*, 87–136.

[8] For some recent examples of merging photoredox chemistry with reductive nickel-catalysis, see; a) J. Yi, S. O. Badir, L. M. Kammer, M. Ribagorda, G. A. Molander, *Org. Lett.* **2019**, *21*, 3346–3351; b) P. Zhou, X. Li, D. Wang, T. Xu, *Org. Lett.* **2021**, *23*, 4683–4687; c) S. H. Lau, M. A. Borden, T. J. Steiman, L. S. Wang, M. Parasram, A. G. Doyle, *J. Am. Chem. Soc.* **2021**, *143*, 15873–15881; d) J. Aragón, S. Sun, D. Pascual, S. Jaworski, J. Lloret-Fillol, *Angew. Chem. Int. Ed.* **2022**, *61*, e202114365.

[9] For some reviews on mechanochemistry, see; a) A. Stolle, T. Szuppa, S. E. S. Leonhardt, B. Ondruschka, *Chem. Soc. Rev.* **2011**, *40*, 2317–2329; b) G.-W. Wang, *Chem. Soc. Rev.* **2013**, *42*, 7668–7700; c) J. Andersen, J. Mack, *Green Chem.* **2018**, *20*, 1435–1443; d) J. L. Howard, Q. Cao, D. L. Browne, *Chem. Sci.* **2018**, *9*, 3080–3094; e) J. L. Do, T. Friščić, *ACS Cent. Sci.* **2017**, *3*, 13–19; f) S. L. James, C. J. Adams, C. Bolm, D. Braga, P. Collier, T. Friščić, F. Grepioni, K. D. M. Harris, G. Hyett, W. Jones, A. Krebs, J. Mack, L. Maini, A. G. Orpen, I. P. Parkin, W. C. Shearouse, J. W. Steed, D. C. Waddell, *Chem. Soc. Rev.* **2011**, *41*, 413–447; g) J. A. Leitch, D. L. Browne, *Chem. Eur. J.* **2021**, *27*, 9721–9726; h) K. J. Ardila-Fierro, J. G. Hernández, *ChemSusChem* **2021**, *14*, 2145–2162; i) M. T. J. Williams, L. C. Morrill, D. L. Browne, *ChemSusChem* **2021**, *15*, e202102157.

[10] For some recent examples of utilizing mechanochemistry in organic synthesis, see; a) W. Riley, A. C. Jones, K. Singh, D. L. Browne, A. M. Stuart, *Chem. Commun.* **2021**, *57*, 7406–7409; b) M. T. J. Williams, L. C. Morrill, D. L. Browne, *ACS Sustainable Chem. Eng.* **2020**, *8*, 17876–17881; c) W. I. Nicholson, A. C. Seastram, S. A. Iqbal, B. G. Reed-Berendt, L. C. Morrill, D. L. Browne, *ChemSusChem* **2020**, *13*, 131–135; d) Z. Zhang, J. Gao, J. J. Xia, G.-W. Wang, *Org. Biomol. Chem.* **2005**, *3*, 1617–1619; e) J. M. Andersen, G. F. Starbuck, *J. Org. Chem.* **2021**, *86*, 13983–13989; f) W. I. Nicholson, F. Barreteau, J. A. Leitch, R. Payne, I. Priestley, E. Godineau, C. Battilocchio, D. L. Browne, *Angew. Chem. Int. Ed.* **2021**, *60*, 21868–21874; *Angew. Chem.* **2021**, *133*, 22039–22045; g) C. Schumacher, C. Molitor, S. Smid, K.-N. Truong, K. Rissanen, C. Bolm, *J. Org. Chem.* **2021**, *86*, 14213–14222; h) J. A. Leitch, H. R. Smallman, D. L. Browne, *J. Org. Chem.* **2021**, *86*, 14095–14101; i) R. Mocci, E. Colacino, L. De Luca C Fattuoni, A. Porcheddu, F. Delogu, *ACS Sustainable Chem. Eng.* **2021**, *9*, 2100–2114.

[11] For some examples of mechanochemical cross-coupling reactions, see; a) A. C. Jones, W. I. Nicholson, H. R. Smallman, D. L. Browne, *Org. Lett.* **2020**, *22*, 7433–7438; b) J. G. Hernández, C. Bolm, *J. Org. Chem.* **2017**, *82*, 4007–4019; c) Z.-J. Jiang, Z.-H. Li, J.-B. Yu, W.-K. Su, *J. Org. Chem.* **2016**, *81*, 10049–10055; d) K. Kubota, H. Ito, *Trends Chem.* **2020**, *2*, 1066–1081; e) K. Kubota, R. Takahashi, H. Ito, *Chem. Sci.* **2019**, *10*, 5837–5842; f) F. Effaty, X. Ottenwaelder, T. Friščić, *Curr. Opin. Green Sustain. Chem.* **2021**, *32*, 100524; g) A. Porcheddu, E. Colacino, L. De Luca, F. Delogu, *ACS Catal.* **2020**, *10*, 8344–8394; h) K. Kubota, T. Seo, K. Koide, Y. Hasegawa, H. Ito, *Nat. Commun.* **2019**, *10*, 111; i) Q. Cao, W. I. Nicholson, A. C. Jones, D. L. Browne, *Org. Biomol. Chem.* **2019**, *17*, 1722–1726.

[12] a) R. Takahashi, P. Gao, K. Kubota, H. Ito, *Chem. Sci.* **2023**, *14*, 499–505; b) Q. Cao, R. T. Stark, I. A. Fallis, D. L. Browne, *ChemSusChem* **2019**, *12*, 2554–2557; c) Y. X. Yin, R. T. Stark, I. A. Fallis, D. L. Browne, *J. Org. Chem.* **2020**, *85*, 2347–2354; d) Q. Cao, J. L. Howard, E. Wheatley, D. L. Browne, *Angew. Chem. Int. Ed.* **2018**, *57*, 11339–11343; *Angew. Chem.* **2018**, *130*, 11509–11513; e) R. Takahashi, A. Hu, P. Gao, Y. Gao, Y. Pang, T. Seo, J. Jiang, S. Maeda, H. Takaya, K. Kubota, H. Ito, *Nat. Commun.* **2021**, *12*, 6691; f) R. A. Haley, A. R. Zellner, J. A. Krause, H. Guan, J. Mack, *ACS Sustainable Chem. Eng.* **2016**, *4*, 2464–2469; g) S. Wada, N. Hayashi, H. Suzuki, *Org. Biomol. Chem.* **2003**, *1*, 2160–2163; h) J. M. Harrowfield, R. J. Hart, C. R. Whitaker, *Aust. J. Chem.* **2001**, *54*, 423–425; i) W. I. Nicholson, J. L. Howard, G. Magri, A. C. Seastram, A. Khan, R. R. A. Bolt, L. C. Morrill, E. Richards, D. L. Browne, *Angew. Chem. Int. Ed.* **2021**, *60*, 23128–23133; *Angew. Chem.* **2021**, *133*, 23312–23317.

[13] a) A. C. Jones, W. I. Nicholson, J. A. Leitch, D. L. Browne, *Org. Lett.* **2021**, *23*, 6337–6341; b) S. Wu, W. Shi, G. Zou, *New J. Chem.* **2021**, *45*, 11269–11274; c) A. C. Jones, M. T. J. Williams, L. C. Morrill, D. L. Browne, *ACS Catal.* **2022**, *12*, 13681–13689.

[14] a) J. L. Howard, Y. Sagatov, L. Repusseau, C. Schotten, D. L. Browne, *Green Chem.* **2017**, *19*, 2798–2802; b) L. Chen, M. Regan, J. Mack, *ACS Catal.* **2016**, *6*, 868–872; c) P. Ying, J. Yu, W. Su, *Adv. Synth. Catal.* **2021**, *363*, 1246–1271.

[15] a) C. Schumacher, J. G. Hernández, C. Bolm, *Angew. Chem. Int. Ed.* **2020**, *132*, 16499–16502; b) H. Lv, X. Xu, J. Li, X. Huang, G. Fang, L. Zheng, *Angew. Chem. Int. Ed.* **2022**, e202206420.

[16] For some examples of nickel-hydride catalysis, see; a) C. F. Liu, X. Luo, H. Wang, M. J. Koh, *J. Am. Chem. Soc.* **2021**, *143*, 9498–9506; b) X. X. Wang, Y. T. Xu, Z. L. Zhang, X. Lu, Y. Fu, *Nat. Commun.* **2022**, *13*; c) Z. Zhang, S. Bera, C. Fan, X. Hu, *J. Am. Chem. Soc.* **2022**, *144*, 7015–7029; d) H. Lv, H. Kang, B. Zhou, X. Xue, K. M. Engle, D. Zhao, *Nat. Commun.* **2019**, *10*, 5025.

[17] A. Guijaro, D. M. Rosenberg, R. D. Rieke, *J. Am. Chem. Soc.* **1999**, *121*, 4155–4167.

RESEARCH ARTICLE

Nickel-Catalyzed Intramolecular Alkene Difunctionalization by Ball-Milling

Adv. Synth. Catal. **2023**, *365*, 1–9

 M. T. J. Williams, L. C. Morrill*, D. L. Browne*

